HIV-1 glycan density drives the persistence of the mannose patch within an infected individual

Karen P. Coss,[1] Snezana Vasiljevic,[2] Laura K. Pritchard,[2] Stefanie A. Krumm,[1] Molly Glaze,[2] Sharon Madzorera,[3,4,5] Penny L. Moore,[3,4,5] Max Crispin,[2]* Katie J. Doores[1]*

[1]Department of Infectious Diseases, Faculty of Life Sciences and Medicine, King's College London, UK.

[2]Oxford Glycobiology Institute and Department of Biochemistry, University of Oxford, UK.

[3]Department of Virology, University of the Witwatersrand, Johannesburg, South Africa

[4]National Institute for Communicable Diseases (NICD) of the National Health Laboratory Service (NHLS), Johannesburg, South Africa.

[5]Centre for the AIDS Programme of Research in South Africa (CAPRISA), University of KwaZulu Natal, Durban, South Africa.

Running title: Longitudinal persistence of the HIV mannose patch

* Address Correspondence to Max Crispin and Katie Doores: max.crispin@bioch.ac.uk (M.C.) and katie.doores@kcl.ac.uk (K.J.D)

Abstract word count: 222

Manuscript word count: 6152

Abstract: The HIV envelope (Env) is extensively modified with host-derived N-linked glycans. The high density of glycosylation on the viral spike limits enzymatic processing resulting in numerous under-processed oligomannose-type glycans. This extensive glycosylation not only shields conserved regions of the protein from the immune system but also act as targets for HIV broadly neutralizing antibodies (bnAbs). In response to the host immune system, the HIV glycan shield is constantly evolving through mutations affecting both the positions and frequencies of potential N-linked glycans (PNGSs). Here, using longitudinal Env sequences from a clade C infected individual (CAP256), we measure the impact of the shifting glycan shield during HIV infection on the abundance of oligomannose-type glycans. By analyzing the intrinsic mannose patch from a panel of recombinant CAP256 gp120s displaying high protein sequence variability and changes in PNGS frequency and positioning, we show that the intrinsic mannose-patch persists throughout the course of HIV infection and correlates with the number of PNGSs. This effect of glycan density on processing state was also supported by the analysis of a cross-clade panel of recombinant gp120 glycoproteins. Together, these observations underscore the importance of glycan clustering for the generation of carbohydrate epitopes for HIV bnAbs. The persistence of the intrinsic mannose patch over the course of HIV infection further highlights this epitope as an important target for HIV vaccine strategies.

Importance:

Development of an HIV vaccine is critical for control of the HIV pandemic, and elicitation of broadly neutralizing antibodies (bnAbs), is likely to be a key component of a successful vaccine response. The HIV Envelope glycoprotein (Env) is covered in an array of host-derived N-linked glycans often referred to as the glycan shield. This glycan shield is a target for many of the recently isolated HIV bnAbs and is therefore under constant pressure from the host immune system leading to changes in both glycan site frequency and location. This study aimed to determine whether these genetic changes impacted the eventual processing of glycans on the HIV Env, and the viruses susceptibility to neutralization. We show that despite this variation in glycan site positioning and frequency over the course of HIV infection, the mannose patch is a conserved feature throughout, making it a stable target for HIV vaccine design.

Introduction:

The HIV envelope glycoprotein (Env) is coated in a dense array of host-derived N-linked glycans. These glycans not only shield conserved regions of the protein from neutralizing antibodies but also act as targets for many of the most broad and potent HIV neutralizing antibodies (1-6). Although HIV Env is glycosylated by the host-cell glycosylation machinery, Env glycosylation has been shown to diverge from that typically observed in mammalian cells (1, 7-15). The dense clustering of PNGSs sterically restricts access of glycan processing enzymes in the ER, which results in a population of under-processed oligomannose-type glycans (7-17) that is a distinctive feature of HIV Env (2) and is independent of producer cell (18). Site-specific analysis of the glycans on recombinant gp120 shows that these oligomannose-type glycans cluster together on the outer domain of gp120 (11, 13, 14, 19, 20) and this cluster is often referred to as the mannose patch and is conserved across Env expression systems (including virion-associated Env, SOSIP trimers and recombinant gp120 monomers) and different geographical clades (7, 15, 17, 18, 20, 21). During expression of both monomeric and trimeric gp120, this mannose population is termed the 'intrinsic mannose patch' (1, 2, 18). In the native trimer, in addition to the intrinsic mannose patch, further steric constraints on glycan processing give rise to the so-called 'trimer-associated mannose patch' (1, 2, 18, 21, 22).

Three main glycan-dependent sites of vulnerability on Env have been identified thus far. These include the N332 glycan/V3 loop which includes the intrinsic mannose patch (recognised by e.g. PGT128, PGT121, 10-1074, PGT135 (5, 23-25)) but also the N160 glycan/V1/V2 loops (e.g. PG9, PG16, PGT145, CAP256-VRC26.25, CH04 (5, 26-28)), and the glycans nearby the gp120/gp41 interface (e.g. PGT151, 35O22, 8ANC195 (29-31)). Protein epitopes such as the CD4 binding site and the membrane proximal external region (MPER) also show some dependence on N-linked glycosylation. For example, the glycans

situated on the rim of the CD4 binding site can modulate neutralization breadth and potency of CD4 binding site bnAbs (22, 32) and perturbation of gp41 glycosylation has been shown to influence the maximum neutralization of MPER bnAb 10E8 (33).

During infection, HIV Env is under constant pressure from the host immune system, in particular neutralizing antibodies, and as such the location and frequency of potential N-linked glycosylation sites (PNGSs) is often changing (3, 34). This observation has led to the concept of the shifting or evolving glycan shield (3). Recent studies aimed at mapping development of HIV broadly neutralizing antibodies (bnAbs) in HIV infected patients has revealed the importance of shifting PNGSs in bNAb development, and shown that immune escape from strain specific antibodies can lead to formation of bNAb epitopes (35-37). For example, Moore et al. showed in an HIV-infected individual that immune pressure against the N334 glycan in a founder virus led to a shift to the conserved N332 glycan position and subsequent development of an N332-dependent bnAb response in that donor (35). Further, removal of the N276 glycan has been shown to confer sensitivity to germline variants of CD4 binding site bnAbs, e.g. VRC01 and NIH45-46, indicating that addition of this glycan as a potential escape mechanism that is critical for development of a broadly neutralizing CD4 binding site antibody response (38).

Studies comparing Env sequences from donor/recipient pairs and large numbers of acute and chronic viruses has shown that clade C transmitted viruses, and to a lesser extent clades A and D, tend to have shorter variable loops and a lower number of PNGSs than chronic viruses (39-43). These trends are observed for both sexual transmission and mother-to-child transmission, however the significance of these differences for HIV transmission is not fully understood. Analysis of longitudinal Env sequences over years of HIV infection has shown that there is an increase in both variable loop length and PNGS

frequency, which is reversed in the later stages of infection (44, 45). It is proposed that this initial increased glycosylation shields neutralizing protein epitopes from the host immune system, which also wanes during late infection (3, 34, 46, 47). Although these studies defined changes in the position and frequency of PNGSs over the course of HIV infection, the effect of these changes on the composition of the glycans present on Env, in particular the persistence of the intrinsic mannose patch, has not yet been determined.

Here we use longitudinal Env sequences from a clade C infected donor, CAP256, to determine the change in glycan shield composition and abundance of oligomannose-type glycans in the intrinsic mannose patch over the course of HIV infection and to relate these changes to variable loop length, frequency of PNGSs and neutralization sensitivity by a panel of HIV bnAbs. The development of the bnAb response in donor CAP256 has been extensively studied and is mediated by bnAbs directed to V1/V2 region on Env (27, 48, 49). This patient was infected with a clade C virus and later became super-infected with a second, unrelated, clade C virus between weeks 13 and 15 leading to Env recombination (27, 48, 49). The viral population early in infection was predominantly made up of the super-infecting (SU) virus with only the V1/V2 and gp41 C-terminus mostly being derived from the primary-infecting (PI) virus (49) but later in infection multiple different recombinant forms existed. Escape from the bnAb response occurred through mutation in V2, in particular at residues R166 and K169 (27, 48, 49).

Here we show that although the number of PNGSs varies by up to five, the intrinsic mannose patch is conserved across all gp120 proteins. However, we observe variation in both the size and composition of the intrinsic mannose patch. We show that there is a strong correlation between frequency of outer domain PNGSs and the abundance of oligomannose-type glycans for both CAP256 gp120s and a cross-clade panel of gp120s

highlighting the importance of glycan density for their restricted access by glycan-processing enzymes. Although there are no strong correlations across the full time period in this donor, a general increase in total PNGSs is observed early in infection and this increase correlates with an increase in oligomannose-type glycans. This is followed by a decline in PNGSs due to loss of glycans at the V3 base and a subsequent decline in oligomannose-type glycans, which was associated with the development of neutralizing antibodies to the C3V4 region. These results demonstrate the persistence of the intrinsic mannose patch over the course of HIV infection and further highlight this region as a stable target for HIV vaccine design strategies.

Materials and Methods:

Cloning and Protein Production

Cloning of the full-length soluble ectodomain of HIV-1 CAP256 gp120s (corresponding to amino acid residues 1 to 507, based on alignment to HxB2 reference strain) into the pHLsec expression vector (50) has previously been described (16, 51). CAP256 Env sequences were published in References (48, 49). The CAP256 proteins were expressed in the 293F variant of HEK 293T cells (ThermoFisher Scientific) that are adapted for suspension culture in 500 mL Erlenmeyer flasks with a vent cap (Corning). Cells were incubated at 37 °C with 5% CO_2, shaking at 137 rpm as recommended by the manufacturer. Briefly, 200 mL cultures were transfected with plasmids (pHLSec) carrying the reporter gene expressing the protein using 293Fectin (ThermoFisher Scientific). Culture supernatants were harvested 5 days after transfection and His-tag proteins were purified by Ni^{2+} affinity purification using a 5 mL HisTrap FF column (GE Healthcare). The nickel-purified proteins were further purified using size exclusion chromatography on a Superdex 200 16/600 column (GE Healthcare). The monomeric fractions were collected, pooled and analysed using SDS-PAGE 4–12% Bis-Tris NuPAGE gel (Invitrogen).

Glycan Profiling: PNGase F release of N-glycans.

N-glycans were released from target glycoprotein immobilised in SDS-PAGE bands using peptide-N-glycosidase F (PNGase F; New England BioLabs) (52). Coomassie-stained gel bands were excised and washed alternately with acetonitrile and water before being dried under vacuum. Gel pieces were rehydrated in 20 mM sodium bicarbonate buffer, pH 7.0, and incubated with PNGase F (1 μL) for 16 h at 37°C. Released glycans were extracted from the gel matrix by 3 washing steps with water.

Fluorescent labelling of N-linked glycans

Released glycans were subsequently fluorescently labelled and purified as previously described (53). PNGase F released N glycans were fluorescently labelled using 2-aminobenzoic acid (2-AA). The labelling mixture comprised 2-AA (30 mg/mL) and sodium cyanoborohydride (45 mg/mL) dissolved in a solution of sodium acetate trihydrate (4% wt/vol) and boric acid (2% wt/vol), in methanol. The labelling mixture (80 μL) was added to each sample (in 30 μL of water) and incubated at 80°C for 1 h. Labelled oligosaccharides were purified using Spe-ed Amide-2 columns (Applied Separations, Allentown, PA) pre-equilibrated with acetonitrile. Before loading, 1 mL 97% acetonitrile (vol/vol) was added to each sample. Loaded samples were then washed with 2 mL 95% acetonitrile (vol/vol) and eluted with 1.5 mL water. Glycans were dried under vacuum prior to UPLC analysis or glycosidase treatment.

Digestion of free, labelled glycans

Glycan samples labelled with 2-AA were digested overnight using Endoglycosidase H (Endo H) (New England Bioscience) in a total volume of 20 μL. Samples were purified with a protein-binding membrane clean-up, using a Ludger vacuum manifold and a multiscreen filter protein-binding plate (MilliPore).

Hydrophilic Interaction Liquid Chromatography -Ultra-Performance Liquid Chromatography

Glycans were separated by hydrophilic interaction liquid chromatography (HILIC)-ultra-high-performance liquid chromatography (UHPLC) using a Waters Acquity system (Waters, USA). Labelled samples were resuspended in 15 µL water and added to a vial with 15 µL 100% acetonitrile. A 2.1 mm × 10 mm Acquity BEH Amide Column (Waters), particle size 1.7 µm, with a programmed gradient was used for separation. Data was acquired and processed with Empower 3 (Waters, USA).

Pseudovirus production and neutralization assays

To produce pseudoviruses, plasmids encoding Env were co-transfected with an Env-deficient genomic backbone plasmid (pSG3ΔEnv) in a 1:2 ratio with the transfection reagent PEI (1 mg/mL, 1:3 PEI:total DNA, Polysciences) into HEK 293T cells (obtained from the American Tissue Culture Collection) (54, 55). Pseudoviruses were harvested 72 hours post transfection for use in neutralization assays. Neutralizing activity was assessed using a single round replication pseudovirus assay with TZM-bl target cells (provided by John Kappes through the NIH AIDS Reagents Repository Program), as described previously (54, 55). Briefly, the antibody was serial diluted in a 96 well flat bottom plate and pre-incubated with virus for 1 hr at 37°C. Cells at a concentration of 20,000 cells/well were added to the virus/antibody mixture and luminescence was quantified 72 hrs following infection via lysis and addition of Bright-Glo™ Luciferase substrate (Promega). Dose-response curves were fitted using nonlinear regression (GraphPad Prism) to determine IC_{50} values.

Antibodies

PGT121, PGT128, PGT135, PG9, b12, PGV04, VRC01, PGT151 and CAP256-VRC26.25 were transiently expressed with the FreeStyle 293 Expression System (Thermofisher Scientific). Antibodies were purified using affinity chromatography (Protein A Sepharose Fast Flow, GE Healthcare) and the purity and integrity was checked by SDS–PAGE.

Correlations/statistics

Correlations were determined using a Pearson correlation and calculated using GraphPad Prism 6.

Preparation of chimeric viruses

223 Chimeric Env containing the C3V4 region were created using an overlapping PCR strategy,
224 and cloned into the pCDNA 3.1D-TOPO vector (Invitrogen) as described previously (56).
225 Chimeric viruses were used to generate pseudoviruses as described above, and assayed for
226 neutralization sensitivity to longitudinal CAP256 plasma (obtained from the CAPRISA cohort).
227 Site-directed mutagenesis was used to delete the N332 glycan within this construct to
228 assess the role of this glycan in mediating escape from plasma nAbs.
229

Results:

Longitudinal analysis of PNGS and V loop length for CAP256 sequences

Env sequences from the CAP256 donor from multiple time points over the course of HIV infection have previously been reported (48, 49). Full Env single genome amplification (SGA) and next generation sequencing of the V1-V3 region (using the MiSeq platform) of viral variants from plasma samples correlated well (48, 57). Here 154 clones from multiple time points were analyzed for their PNGS position and frequency as well as their variable loop lengths. Previous studies have reported an increase in PNGSs and variable loop lengths over the course of HIV infection (44, 45). Therefore, we first determined whether these trends were observed in CAP256 (Figure 1). We first considered the changes in variable loop lengths over time. Although there is variation in both the individual and total variable loop lengths during the course of infection, there are no notable correlations. However, there was a weak negative correlation between total V loop length and weeks post infection up until week 94 (r = -0.2496, p = 0.0039) (Figure 1A). We next considered PNGS frequency. For all CAP256 Env sequences the frequency of gp41 PNGSs remained constant at 4 and the location of these sites did not alter during the course of infection (Figure 2). The frequency of total PNGSs for gp120 ranged from 22 to 28, with the primary infecting (PI) and super-infecting (SU) viruses having mostly 23 and 25 PNGSs respectively (Figure 1B). The majority of variation in PNGS frequency occurred within variable loops, in particular the V1/V2 loops and glycan sites positioned at the base of the V3 loop (N295, N332 and N334). When the frequency of PNGSs was plotted against the number of weeks post infection a weak positive correlation (r = 0.21, p = 0.01) was observed. However, as the glycan shield is a dynamic entity that is under constant pressure from the host immune system we also looked for correlations over smaller time periods. In this donor a strong positive correlation (r = 0.64, p < 0.0001) was observed up until week 94, after which the number of PNGSs declined and the correlation weakened (Figure 1B). This decrease corresponds

predominantly to the loss of glycan sites at positions N295 and N332. A slight decrease in PNGSs around weeks 30 to weeks 34 was also observed which corresponded to loss of V1/V2 loop PNGSs, and the N289 or N295 glycan sites (Figure 1B). Interestingly, this is the first time point that the V1/V2-specific antibody response was detected and subsequently led to a sudden increase in viral diversification (48, 57). A similar trend was observed for PNGSs on the outer domain of gp120 up until week 94 (OD, residues 252-482), however there was no correlation over the full time period (Figure 1C). In summary, in the CAP256 donor there is a general trend towards increasing PNGSs early in infection that decreases at the latest time point (week 176), which is consistent with previous studies (44, 45). However, there is still considerable variation between single viruses at a given time point, (e.g. at week 176 the total number of PNGSs differs by 4 (Figure 1B)) enabling us to assess the prevalence of the intrinsic mannose patch.

The intrinsic mannose patch is present on gp120 throughout HIV infection in donor CAP256.

To determine changes in the composition of the HIV glycan shield and abundance of oligomannose-type glycans within the intrinsic mannose patch over the course of infection, the gp120 region of 24 CAP256 Envs from different timepoints were recombinantly expressed. The selected clones were chosen to represent major clades within a phylogenetic tree based on single genome amplification. This smaller sample of CAP256 Envs displayed a similar correlation between weeks post infection and PNGS frequency as for the 154 Env sequences (Figure 1D-F) and their PNGS position and frequency are reported in Figure 2. We were particularly interested in the abundance of oligomannose-type glycans of the intrinsic mannose patch as these glycans form part of the epitopes of a number of the most broad and potent HIV bnAbs (e.g. PGT121, PGT128 and PG9) (5, 25, 58, 59). As we have previously shown that the intrinsic mannose patch of recombinant

gp120 captures much of the steric constraints exhibited by these glycans in the context of the trimer (including SOSIP trimers) (7, 15, 17, 18, 22), monomeric gp120 was used as a useful model of this viral feature. Residues 1 to 517 were cloned into a recombinant expression vector (pHLSec) (50, 51) and expressed in HEK 293F cells for glycan profiling (we have previously shown that the mannose patch is largely independent of producer cell (17, 18)). The protein constructs included a C-terminal hexa-histidine tag so that nickel affinity purification could be used to avoid potential bias associated with other glycan-specific purification methods such as lectins. Proteins were purified first using His-tag affinity chromatography followed by size exclusion chromatography (SEC) to remove aggregates. Purified proteins were then run on a non-reducing SDS-PAGE gel and the monomeric gp120 band excised for glycan analysis. N-linked glycans were released using PNGase F, fluorescently labeled and analyzed by HILIC-UPLC. The percentage of oligomannose glycans was assessed by integration of chromatograms pre- and post-Endo H digestion generating specific percentage areas for the oligomannose glycans (Figure 3A). It was then possible to assign structures based on previous analysis (16, 18).

All gp120 samples displayed an intrinsic mannose-patch, however the population of oligomannose-type glycans varied from 29.3% to 47.6% (Table S1). The percentage change in oligomannose levels between gp120 94wks.A3, that has the highest number of PNGSs (a total of 28), and 6wks_PI, that has the fewest number of PNGSs (a total of 23), is 27% and 212% for $Man_{5\text{-}9}GlcNAc_2$ and $Man_9GlcNAc_2$ respectively. Gp120 94wks.A3 has additional PNGSs in V1 (N135, N160), in C2 (N230), in C3 (N362) and V4 (N406, N413) whereas 6wks_PI has an additional PNGS in C4 (N442). We have previously measured the decrease in oligomannose-type glycans on BaL gp120 when one or two PNGSs were removed through Asn to Ala substitution (16). The largest effect was observed for the N295A/N386A double mutant where the percentages of $Man_{5\text{-}9}GlcNAc_2$ and $Man_9GlcNAc_2$ decreased by

27% and 71% respectively. Therefore, compared to our previous observations, the difference in oligomannose-type glycan abundance for 94wks.A3 and 6wks_PI is relatively small considering these recombinant proteins differ by five PNGSs (16) but the difference in $Man_9GlcNAc_2$ structures is much higher. This observation is not unexpected given the position of two of the additional PNGSs are on the gp120 OD where PNGSs are tightly clustered (see discussion below). This therefore suggests that there are regions on gp120 where multiple glycans can be removed with little impact on glycan processing of the intrinsic mannose patch and it is the local density of PNGSs that determines the extent of glycan processing.

Abundance of oligomannose-type glycans correlates with density of PNGSs.

To determine factors that might influence the abundance of specific oligomannose-type glycans on gp120 we correlated the percentage of $Man_{5-9}GlcNAc_2$ glycans with the total PNGSs on gp120 (Figure 3B). A positive correlation was observed (r = 0.486, p = 0.016) and this correlation became more significant when only $Man_9GlcNAc_2$ glycan abundance was considered (r = 0.695, p = 0.0002). When the percentage $Man_{5-9}GlcNAc_2$ and $Man_9GlcNAc_2$ were correlated with the frequency of PNGSs present only on the outer domain (OD) of gp120 then a strong positive correlation was observed for both $Man_{5-9}GlcNAc_2$ and $Man_9GlcNAc_2$ (r = 0.752, p =< 0.0001, and r = 0.717, p =< 0.0001 respectively) (Figure 3C). The gp120 OD PNGSs include many of the sites shown to be oligomannose-type in site-specific analysis studies (8, 11, 14, 22, 60). Further, the recent crystal structures of the BG505 SOSIP.664 recombinant trimer showed the PNGSs in this region cluster tightly on the surface of Env (58, 61). Therefore an increase in PNGSs on the outer domain of gp120 will likely further restrict access of the glycan-processing enzymes leading to an increase in oligomannose-type glycans on gp120 and the size of the intrinsic mannose patch (7, 17). Interestingly, some gp120s that have the same positioning and frequency of PNGS still

showed differences in percentage of oligomannose-type glycans highlighting the role protein sequence may also play in determining the structure of the HIV glycan shield. For example, 59wks.2a and 59wks.10b have identical PNGSs yet the percentage of oligomannose-type glycans differs by 3.6%.

Longer variable loop lengths might be expected to decrease the density of PNGSs and lead to a higher degree of glycan-processing and therefore a reduction in oligomannose-type glycans. Although the CAP256 gp120 sequences differed in combined variable loop length by up to 20 amino acids, no correlation was observed between oligomannose abundance and variable loop length (Figure 3D) suggesting that positioning of specific glycan sites is most critical to oligomannose abundance.

Abundance of oligomannose-type glycans correlates with density of outer-domain PNGSs for a cross-clade panel of gp120s.

To determine whether the correlation between the number of PNGSs on the outer-domain of gp120 and the abundance of oligomannose-type glycans was a general feature for HIV Env across geographical clades, a panel of 29 gp120s were cloned, expressed and purified as described above. The panel included gp120s from clades A, B, C, AE and G, of which five were transmitted/founder viruses. All isolates tested were found to possess a significant population of oligomannose-type glycans ranging from 23.8% to 50.5% (Figure 4 and table S2). When the abundance of oligomannose-type glycans was correlated with the total number of PNGSs (ranging from 21 to 28), no significant correlation was observed (Figure 4A). However, a significant correlation was observed between the frequency of OD PNGSs (ranging from 12-17) and oligomannose abundance, similar to that seen for the CAP256 samples (r = 0.4692, p = 0.010; Figure 4B). No significant correlations were observed between total PNGSs or OD PNGSs and $Man_9GlcNAc_2$ (data not shown). These data further

support the notion that a high density of PNGSs on OD restricts glycan-processing enzymes leading to a higher population of under-processed oligomannose-type glycans. These data also suggest that it is local glycan density that has the largest impact on glycan processing rather than overall glycan density. Interestingly, the specific occupancy and composition of individual sites was not assessed here but this could be an informative extension in future studies.

While there are variations in the percentage of certain oligomannose structures between the clades (clades C and G having less $Man_9GlcNAc_2$ structures, and clade C having less $Man_8GlcNAc_2$ structures), the overall abundance of oligomannose glycans is fairly similar (Figure 4C and 4D). Clade C has the lowest total percentage oligomannose (35.5%), yet when compared to clade B, with one of the highest percentages and lowest SD (38.5%, SD 4.98), there is no significant difference between the two (Figure 4C), although this difference might become more significant if more gp120s were studied. Considering the correlation between outer-domain PNGSs and $Man_{5-9}GlcNAc_2$ it is likely that loss of specific sites between clades is responsible for the differences in specific glycan abundance. This is particularly relevant for clade C viruses that typically lack the N295 glycan site (62, 63), a PNGS we have previously shown to stabilize the mannose patch from glycan processing (16). However, while there are some differences in the structures, the total level of oligomannose-type glycans remains similar between clades, indicating the overall stability and conserved nature of the mannose patch.

Correlation of oligomannose-type glycans with time post-infection

We next examined how the size of the intrinsic mannose patch changes over the course of HIV infection. We first correlated the percentage of oligomannose-type glycans against the weeks post infection but no correlation was observed (Figure 5A). As the glycan shield is a

386 dynamic entity that is under constant pressure from the host immune system we also looked
387 for correlations over smaller time periods to reflect this. We observed correlations between
388 $Man_{5-9}GlcNAc_2$ and $Man_9GlcNAc_2$ abundance and weeks post infection up until week 94 (r =
389 0.513, p = 0.025 and r = 0.666, p = 0.0019 respectively, Figure 5A) similar to that seen for
390 changes in PNGS frequency over time. The abundance of oligomannose-type glycans then
391 largely persists but exhibits some variation due to sensitivity to loss of PNGSs at the base of
392 V3, in particular at positions N295 and N332/N334 (Figure 2).
393
394 To analyze the changes in Env glycan composition over time in more detail, we next
395 determined the percentage change in total oligomannose-type glycans ($Man_{5-9}GlcNAc_2$) and
396 $Man_9GlcNAc_2$ individually for each gp120 clone (Figure 5B). As the viral population early in
397 infection was predominantly made up of the SU virus, with only the V1/V2 and gp41 C-
398 terminus mostly being derived from the PI virus, changes in total $Man_{5-9}GlcNAc_2$ and
399 $Man_9GlcNAc_2$ composition were considered in relation to the SU virus. Although the
400 mannose patch is present on all CAP256 proteins studied, the changes in $Man_{5-9}GlcNAc_2$
401 and $Man_9GlcNAc_2$ can vary for individual clones at a given time point. Generally, a large
402 increase in oligomannose-type glycans was due to increases in $Man_8GlcNAc_2$ and
403 $Man_9GlcNAc_2$ early stage glycan structures (Figure 5B and Table S1) further suggesting
404 increased density in PNGSs leads to reduced glycan processing. For example, gp120s from
405 weeks 59 and 94, which had the highest oligomannose-type glycan abundance (44.0-47.6%),
406 had 28.4-30.4% $Man_{8-9}GlcNAc_2$ structures. Interestingly, previous analysis of glycan site
407 mutants showed that the presence of $Man_9GlcNAc_2$ was particularly dependent on multiple
408 stabilizing interactions with neighbouring glycans (16).
409
410 **Abundance of oligomannose-type glycans does not correlate with neutralization**
411 **potency of HIV bnAbs.**

412 We next wanted to determine whether the structure of the HIV glycan shield, in particular the
413 abundance of oligomannose-type glycans, might influence the potency of neutralization by a
414 panel of HIV bnAbs. We therefore determined the IC_{50} values for intrinsic mannose patch
415 binding bnAbs PGT121, PGT128 and PGT135, V1/V2 loop bnAbs PG9 and several of
416 CAP256-VRC26 antibody lineage, cleavage-specific bnAb PGT151, and CD4 binding site
417 bnAbs PGV04, VRC01 and llama antibody VHH J3 (Table S3). When the IC_{50} values were
418 correlated with the abundance of oligomannose-type glycans no significant correlations were
419 observed for any bnAbs (Figure 6), although a general weak trend for increasing IC_{50} values
420 with increasing oligomannose-type glycans was observed for some bnAbs. Generally, the
421 ability of a bnAb to neutralize a viral variant was dependent on the presence of key contact
422 glycan sites such as N160 or N332. The majority of viruses were resistant to PGT135
423 neutralization and viruses lacking the N332 glycan site, and in one case the N295 glycan
424 site, were resistant to PGT128. PGT121 was able to neutralize all but two viruses. PG9
425 could not neutralize viruses lacking the N160 glycan site or viruses with a glutamic acid at
426 position 169 (Figure 2, Figure 6 and Table S3) (48) whereas CAP256-VRC26 lineage bnAbs
427 were dependant on protein residues in V1 for neutralization (27). Interestingly, none of
428 CAP256-VRC26 lineage bnAbs isolated over several different time points throughout
429 infection (weeks 119, 159, 193 and 206) showed any correlation with oligomannose
430 abundance suggesting increasing the size of the mannose-patch is not a direct mechanism
431 of escape against the autologous antibodies in this donor. For PGT151, although all viruses
432 contained the key glycan sites and residues thought to be required for neutralization (N611,
433 N637 and E647) some viruses were nonetheless resistant to PGT151 neutralization.
434 Potency for the CD4 binding-site bnAbs PGV04, VRC01 and J3, which do not contact
435 glycans, generally did not correlate with the level of oligomannose-type glycans. As N-linked
436 glycans are positioned around the edge of the CD4 binding site, the changes in bulk glycan
437 structures observed may not be occurring in this region of gp120 and therefore not impact

438 on CD4 binding-site bnAbs but site-specific glycan analysis would be required to determine
439 this. Interestingly, the smaller single chain llama antibody, J3, had the smallest variation in
440 IC_{50} values. Therefore, the abundance of oligomannose-type glycans in the intrinsic
441 mannose patch does not impact on potency of neutralization and suggests Env sequences
442 from any time point during infection, provided they have the key contact glycan sites, would
443 be suitable HIV immunogens.
444
445 **Anti-C3/V4 nAbs may be responsible for loss of PNGSs at week 176.**
446 The loss of glycan sites at the base of the V3 loop at week 176 suggested that neutralizing
447 antibodies might be exerting selection pressure against this region that is leading to loss of
448 PNGSs and a decrease in abundance of oligomannose-type glycans. To assess whether
449 this region was a target of nAbs, we created a chimeric Env from the 176wks.4 Env, which
450 had already escaped the high titer V2 responses that dominate CAP256 plasma (49). Using
451 overlapping PCR, we transferred the C3V4 region from the sensitive 15wks_SU virus into
452 the resistant backbone and tested this chimeric Env (15wks_SU C3V4) against longitudinal
453 plasma (Figure 7). Anti-C3V4 antibodies at titers greater than 1:100 were detected from 42
454 weeks post-infection persisting at least until 94 weeks at which time point an additional
455 specificity emerges. To determine whether the anti-C3V4 antibodies were directed against
456 the N332 glycan site in particular we next used site-directed mutagenesis to make an Asn to
457 Ala substitution at the N332 glycan site (15wks_SU C3V4 N332A). A decrease in serum
458 titres was observed indicating that some of the C3V4-antibody response is directed against
459 the N332 epitope (Figure 7). The presence of anti-C3V4 nAbs suggests that nAbs against
460 this region can elicit a selective pressure that results in loss of V3 loop glycans and a
461 subsequent decrease in oligomannose-type glycans.
462

Discussion:

It is clear that the HIV glycan shield is under constant pressure from the host immune system. Here we use longitudinal Env sequences from a chronically infected HIV patient to characterize the changes in the structure of the HIV glycan shield during the course of HIV infection, in particular the persistence and composition of the intrinsic mannose-patch. We show that in the CAP256 donor the mannose patch (Figure 8A) persists throughout infection despite the variation in PNGS position and frequency (Figure 8B). In this donor there is an increase in PNGSs and oligomannose-type glycans within the intrinsic mannose patch over the course of infection up until week 94. This increase correlates with the frequency of PNGSs on the outer domain. Thereafter, there is a reduction in PNGSs at the base of the V3 and a corresponding reduction in oligomannose-type glycans by week 176, likely a consequence of viral escape from a *de novo* neutralizing response to the C3V4 region. Although this study focuses on only one donor, these findings give insight into the composition and conservation of the intrinsic mannose patch under immune pressure and highlights this epitope as an important target for HIV vaccine design strategies.

Our previous studies have shown that the glycosylation of HIV Env is determined by both protein-directed effects, arising from the 3-dimensional protein structure, and cell-directed effects, arising from the cell-type the protein is expressed in (2, 17, 18). The protein-directed effects give rise to a patch of under-processed oligomannose-type glycans on the outer domain of gp120 that forms a non-self epitope targeted by HIV bnAbs. We show that despite the variation in protein sequence and positioning and frequency of PNGSs, the intrinsic mannose patch is highly conserved during the course of infection in the CAP256 donor and therefore represents a stable target for vaccine design. However, the intrinsic mannose patch varies in both overall size and distribution of glycans within the oligomannose series ($Man_{5\text{-}9}GlcNAc_2$) and this most strongly correlates with the density of PNGSs present on the

OD of gp120. This trend was also observed, although to a lesser extent, for a cross-clade panel of gp120 and highlights the role protein sequence might also play in determining the structure of the HIV glycan shield. These data support our previous conclusions that the high-density of PNGSs restricts glycan-processing enzymes from trimming and processing N-linked glycans within this region (7, 15, 16, 18, 64). Interestingly, it seems to be the local glycan density rather than then overall glycan density that has the biggest impact of size and composition of the mannose-patch. Although Env sequences vary by up to 5 PNGSs it is clear that it is mainly PNGSs within and around the outer domain of gp120 that affects the size and distribution of oligomannose-type glycans within the intrinsic mannose patch. The potency of neutralization by a panel of HIV bnAbs is not affected by the variation in mannose patch composition but is dependent on the presence of certain key PNGSs. This suggests that PNGSs on gp120 are sufficiently high density that the natural variation in Env occurring throughout infection has minimal impact on glycan processing such that the mannose-patch, which is intrinsic to both monomer and trimer is always present. Therefore, the density of glycans on gp120, even at the lowest density, is sufficient to maintain the steric restriction necessary to impede mannosidase processing. This is consistent with previous observations suggesting that minimal glycan-glycan interactions are required to prevent processing to complex-type glycans (16). In addition, this effect may be further compounded by the trimer-associated restriction to processing not captured by our monomeric gp120 model (1, 2, 18, 22). Although several studies have reported more compact transmitter clade C and A viruses (39, 40), with shorter V1-V4 loop length, this does not appear to impact the glycosylation of gp120s from the CAP256 donor.

The most dramatic changes to the HIV glycan shield of CAP256 gp120 occurs when glycans at the base of the V3 loop are added or deleted. This is supported by our previous studies showing that deletion of glycans within the region for $gp120_{BaL}$ had the largest impact on

515 oligomannose-type glycan abundance due to disruption of glycan microclusters within the
516 outer domain (16). We have shown that some of the changes occurring in PNGS position
517 and frequency of CAP256 gp120, and subsequently oligomannose abundance, at week 176
518 post infection are likely a result of a new wave of neutralizing antibodies targeting the C3V4
519 region, including the N332 glycan. These data may suggest the selective pressure of
520 neutralizing Abs targeting the intrinsic mannose patch would have the biggest effect on
521 shaping the glycan structures present on the HIV glycan shield. Unfortunately, full-length
522 Envs from later time-points were not available but as the C3/V4 specific response arose
523 after approximately 75 weeks, any additional destabilization of the intrinsic mannose patch is
524 likely to occur within the time frame studied. It is possible that if a similar study was carried
525 out in a donor who developed bnAbs against another epitope, such as the CD4 binding site,
526 less variation in OD PNGS frequency would occur and thus a smaller variation in
527 oligomannose-type glycans would be observed over the course of infection.
528
529 Desaire and colleagues have previously compared the glycosylation of recombinant gp120
530 from transmitted/founder (t/f) viruses and chronic viruses (60). They conclude that t/f Envs
531 are more similar to each other than to their corresponding chronic viruses, with t/f Envs
532 having distinct glycosylation patterns consisting of a higher degree of oligomannose and
533 sialylated glycans, and a lower site occupancy (60). However, the study was limited as only
534 two t/f and two chronic viruses were studied and these viruses were not derived from the
535 same donors. Indeed, comparison of oligomannose levels on the t/f and chronic viruses in
536 our gp120 panel showed no significant differences. By using longitudinal virus sequences
537 we are able to show that over the course of infection in the CAP256 individual there is an
538 increase in PNGSs and a corresponding increase in oligomannose-type glycans that is
539 subsequently reduced by the pressure of neutralizing antibodies. Although the PI and SU
540 gp120s have lower levels of oligomannose-type glycans (35.3% and 36.4% respectively)

than the majority of gp120s from later time points, there are viruses within the quasispecies that have lower levels of oligomannose glycans, e.g. 38wks.38 and 48wks.10 having 32.7% and 35.5% oligomannose-type glycans respectively. What would be interesting to determine is the glycosylation of Envs within the HIV infected donor who transmitted the viruses to the CAP256 donor, however these samples are not available.

Although we have only studied one HIV infected individual in detail, a number of studies have shown t/f viruses have a lower frequency of PNGSs (39-43). Whether there would be a benefit for t/f viruses to have a reduced frequency of PNGSs and subsequently display a lower proportion of oligomannose-type glycans is unclear. In relation to HIV transmission, studies have shown the importance of the interaction of DC-SIGN receptors on DCs in mucosal tissues for transfection of CD4+ T cells is strongly dependent on the presence of oligomannose structures (65-67). In relation to infectivity, reduction of complex-type glycans on HIV virions (through use of glycosidase inhibitors or a GnTI-deficient cell line) reduced the infectivity of the virus but enhanced trans-infection of peripheral blood lymphoctyes (32, 68). In relation to Env immunogenicity, studies have shown that removal or occlusion of mannose residues from the surface of gp120 can enhance the immune response against HIV due to reduced interactions with immunosuppressive receptors such as the mannose-receptor (69-71). Taken together, these studies might suggest a higher abundance of oligomannose-type glycans would be more beneficial for transmitted viruses. It is therefore possible that the reduced oligomannose levels in the PI and SU viruses is only a consequence of lower PNGSs and does not give a virus competitive advantage at the point of transmission. However, there may be a trade-off between viral infectivity and host recognition. Regardless, in terms of vaccine design, Env based immunogens with a lower abundance of oligomannose-type glycans (from the CAP256 donor this would be Envs from

earlier time-points) might give a stronger immune response as suggested by the studies described above (69-71).

In summary, although in the CAP256 donor there are changes in both frequency and positioning of PNGSs due to immune pressure, the intrinsic mannose patch remains a stable feature of HIV Env and is present throughout the course of HIV infection. The density of PNGSs on the outer domain of gp120 can influence the size and composition of the intrinsic mannose patch but these differences do not affect the neutralization sensitivity of a panel of HIV bnAbs. These findings, in addition to our previous observations showing the presence of the intrinsic mannose patch to be independent of producer cell, further highlights the mannose patch as a stable target for HIV vaccine design.

Acknowledgements

We thank Jinal Bhiman for the original cloning of the CAP256 Env variants from patient samples. We thank Hajer Mohammed for help with cloning of some of the gp120 expression constructs.

Figure Legends:

Figure 1: Correlation between weeks post infection and A) total length of variable loops (V1-V5), B) total PNGSs on gp120, and C) PNGSs on gp120 outer domain (residues 252-482). 154 previously published Env sequences over multiple time-points were used in the analysis (48). Correlation between weeks post infection and D) total length of variable loops (V1-V5), E) total PNGSs on gp120, and F) PNGSs on gp120 outer domain (residues 252-482) for the 24 recombinantly expressed gp120s. The primary infecting virus (PI) and super infecting virus (SU) are at weeks 6 and 15 respectively. Correlations were assessed by Pearson analyses: p-values and r-values are indicated between weeks 6 to 94 and between weeks 6 to 176 (All). Note that some of the sequences have identical PNGS, OD PNGS and V loop lengths and these points are overlaid.

Figure 2: Summary of PNGSs for 24 representative CAP256 Env clones that were expressed recombinantly. Total PNGSs on gp160, gp120, the outer domain, V1/V2, V3/V4 or gp41 are calculated for each clone. Clones are grouped together according to the time they were isolated. A white box indicates a PNGS is absent and a blue box indicates a PNGS is present.

Figure 3: A) HILIC-UPLC spectrum of fluorescently labelled N-linked glycans released from 48wks.17 gp120 using PNGase F. This is presented as an example of the quantification methodology. The green trace is a spectrum of released glycans and the white trace is the spectrum for Endo H treated glycans. Overlaying of the spectra results in the glycans sensitive to Endo H being displayed as green. The percentage of oligomannose glycans was assessed by integration of chromatograms pre- and post-Endo H digestion generating specific percentage areas for the oligomannose glycans. The oligomannose glycans are highlighted (M5-M9, $Man_{5-9}GlcNAc_2$). Correlation between abundance of oligomannose-type

612 glycans ($Man_{5-9}GlcNAc_2$ and $Man_9GlcNAc_2$) and B) total PNGSs on gp120, C) PNGSs on
613 gp120 outer domain (residues 252-482) and D) total variable loop lengths. Correlations were
614 assessed by Pearson analyses: p-values and r-values are indicated.
615
616 **Figure 4:** Correlation between the percentage of oligomannose-type glycans ($Man_{5-9}GlcNAc_2$)
617 and A) total PNGSs on gp120 and B) PNGSs on the outer domain of gp120
618 (residues 252-482) for a cross-clade panel of gp120 glycoproteins. Each point is coloured
619 depending on the HIV clade (A (n=7), B (n=8), C (n=6), AE (n=4) and G (n=4)). Correlations
620 were assessed by Pearson analyses: p-values and r-values are indicated. Cross clade
621 gp120 panel differences for C) Man_5-Man_9 and Man_9, and D) Total PNGSs, and OD PNGSs.
622 Error bars represent standard deviation. Mann-Whitney test was used to show that there
623 were no significant differences between the groups.
624
625 **Figure 5:** A) Correlation between weeks post infection and abundance of $Man_{5-9}GlcNAc_2$
626 and $Man_9GlcNAc_2$. B) Percentage change in $Man_{5-9}GlcNAc_2$ and $Man_9GlcNAc_2$ compared to
627 the SU virus for each CAP256 gp120 clone studied (% change = ((%CAP-%SU)/%SU)*100).
628 Correlations were assessed by Pearson analyses: p-values and r-values are indicated.
629
630 **Figure 6:** Correlation between potency of neutralization (IC_{50} values) and the percentage of
631 oligomannose-type glycans for a panel of HIV bnAbs. A) N332-dependent (intrinsic mannose
632 patch binding) bnAbs, B) CD4 binding site bnAbs, C) PGT151 and D) N160 V1/V2 loop
633 bnAbs. Correlations were assessed by Pearson analyses. IC_{50} values are reported in Table
634 S4.
635
636 **Figure 7:** Kinetics of the C3V4 neutralizing antibody response in CAP256. Titres are shown
637 using the CAP256 176wks.4 virus (black) and chimeric Envs containing only the C3V4

region of the sensitive SU virus (15wks_SU C3V4, red) and an N332A variant (15wks_SU C3V4 N332A, orange). Anti-C3V4 antibodies at titers greater than 1:100 were detected from 42 weeks post-infection persisting at least until 94 weeks. The anti-C3V4 antibodies show some N332A dependence. Titres are indicated as plasma ID_{50} versus weeks post-infection.

Figure 8: Schematic representation of evolving HIV glycan shield. A) Structure of BG505 SOSIP.644 trimer showing the presence of the intrinsic mannose patch (IMP, green) present on one of the three gp120 monomers (22, 72). B) Cartoon representation of the longitudinal evolution of the intrinsic mannose patch on gp120. Despite the changes in position and frequency of PNGSs on gp120, the intrinisic mannose patch persists throughout infection in this individual. The hashed area represents the intrinsic mannose patch from one gp120 monomer.

References:

1. **Crispin M, Doores KJ.** 2015. Targeting host-derived glycans on enveloped viruses for antibody-based vaccine design. Curr Opin Virol **11C:**63-69.
2. **Doores KJ.** 2015. The HIV glycan shield as a target for broadly neutralizing antibodies. Febs J **282:**4679-4691.
3. **Wei X, Decker JM, Wang S, Hui H, Kappes JC, Wu X, Salazar-Gonzalez JF, Salazar MG, Kilby JM, Saag MS, Komarova NL, Nowak MA, Hahn BH, Kwong PD, Shaw GM.** 2003. Antibody neutralization and escape by HIV-1. Nature **422:**307-312.
4. **Scanlan CN, Pantophlet R, Wormald MR, Ollmann Saphire E, Stanfield R, Wilson IA, Katinger H, Dwek RA, Rudd PM, Burton DR.** 2002. The broadly neutralizing anti-human immunodeficiency virus type 1 antibody 2G12 recognizes a cluster of alpha1-->2 mannose residues on the outer face of gp120. J Virol **76:**7306-7321.
5. **Walker LM, Huber M, Doores KJ, Falkowska E, Pejchal R, Julien JP, Wang SK, Ramos A, Chan-Hui PY, Moyle M, Mitcham JL, Hammond PW, Olsen OA, Phung P, Fling S, Wong CH, Phogat S, Wrin T, Simek MD, Koff WC, Wilson IA, Burton DR, Poignard P.** 2011. Broad neutralization coverage of HIV by multiple highly potent antibodies. Nature **477:**466-470.
6. **Scanlan CN, Offer J, Zitzmann N, Dwek RA.** 2007. Exploiting the defensive sugars of HIV-1 for drug and vaccine design. Nature **446:**1038-1045.
7. **Doores KJ, Bonomelli C, Harvey DJ, Vasiljevic S, Dwek RA, Burton DR, Crispin M, Scanlan CN.** 2010. Envelope glycans of immunodeficiency virions are almost entirely oligomannose antigens. Proc Natl Acad Sci U S A **107:**13800-13805.
8. **Go EP, Irungu J, Zhang Y, Dalpathado DS, Liao HX, Sutherland LL, Alam SM, Haynes BF, Desaire H.** 2008. Glycosylation site-specific analysis of HIV envelope proteins (JR-FL and CON-S) reveals major differences in glycosylation site occupancy, glycoform profiles, and antigenic epitopes' accessibility. J Proteome Res **7:**1660-1674.
9. **Mizuochi T, Spellman MW, Larkin M, Solomon J, Basa LJ, Feizi T.** 1988. Structural characterization by chromatographic profiling of the oligosaccharides of human immunodeficiency virus (HIV) recombinant envelope glycoprotein gp120 produced in Chinese hamster ovary cells. Biomed Chromatogr **2:**260-270.
10. **Mizuochi T, Spellman MW, Larkin M, Solomon J, Basa LJ, Feizi T.** 1988. Carbohydrate structures of the human-immunodeficiency-virus (HIV) recombinant envelope glycoprotein gp120 produced in Chinese-hamster ovary cells. Biochem J **254:**599-603.
11. **Zhu X, Borchers C, Bienstock RJ, Tomer KB.** 2000. Mass spectrometric characterization of the glycosylation pattern of HIV-gp120 expressed in CHO cells. Biochemistry **39:**11194-11204.
12. **Mizuochi T, Matthews TJ, Kato M, Hamako J, Titani K, Solomon J, Feizi T.** 1990. Diversity of oligosaccharide structures on the envelope glycoprotein gp 120 of human immunodeficiency virus 1 from the lymphoblastoid cell line H9. Presence of complex-type oligosaccharides with bisecting N-acetylglucosamine residues. J Biol Chem **265:**8519-8524.
13. **Geyer H, Holschbach C, Hunsmann G, Schneider J.** 1988. Carbohydrates of human immunodeficiency virus. Structures of oligosaccharides linked to the envelope glycoprotein 120. J Biol Chem **263:**11760-11767.
14. **Leonard CK, Spellman MW, Riddle L, Harris RJ, Thomas JN, Gregory TJ.** 1990. Assignment of intrachain disulfide bonds and characterization of potential glycosylation sites of the type 1 recombinant human immunodeficiency virus

envelope glycoprotein (gp120) expressed in Chinese hamster ovary cells. J Biol Chem **265:**10373-10382.

15. **Bonomelli C, Doores KJ, Dunlop DC, Thaney V, Dwek RA, Burton DR, Crispin M, Scanlan CN.** 2011. The Glycan Shield of HIV Is Predominantly Oligomannose Independently of Production System or Viral Clade. PLoS One **6:**e23521.
16. **Pritchard LK, Spencer DI, Royle L, Bonomelli C, Seabright GE, Behrens AJ, Kulp DW, Menis S, Krumm SA, Dunlop DC, Crispin DJ, Bowden TA, Scanlan CN, Ward AB, Schief WR, Doores KJ, Crispin M.** 2015. Glycan clustering stabilizes the mannose patch of HIV-1 and preserves vulnerability to broadly neutralizing antibodies. Nat Commun **6:**7479.
17. **Pritchard LK, Harvey DJ, Bonomelli C, Crispin M, Doores KJ.** 2015. Cell- and Protein-Directed Glycosylation of Native Cleaved HIV-1 Envelope. Journal of virology **89:**8932-8944.
18. **Pritchard LK, Vasiljevic S, Ozorowski G, Seabright GE, Cupo A, Ringe RP, Kim HJ, Sanders RW, Doores KJ, Burton DR, Wilson IA, Ward AB, Moore JP, Crispin M.** 2015. Structural constraints determine the glycoyslation of HIV-1 envelope trimers. Cell Rep **11:**1604-1613.
19. **Go EP, Liao HX, Alam SM, Hua D, Haynes BF, Desaire H.** 2013. Characterization of host-cell line specific glycosylation profiles of early transmitted/founder HIV-1 gp120 envelope proteins. J Proteome Res **12:**1223-1234.
20. **Go EP, Herschhorn A, Gu C, Castillo-Menendez L, Zhang S, Mao Y, Chen H, Ding H, Wakefield JK, Hua D, Liao HX, Kappes JC, Sodroski J, Desaire H.** 2015. Comparative Analysis of the Glycosylation Profiles of Membrane-Anchored HIV-1 Envelope Glycoprotein Trimers and Soluble gp140. J Virol **89:**8245-8257.
21. **Panico M, Bouche L, Binet D, O'Connor MJ, Rahman D, Pang PC, Canis K, North SJ, Desrosiers RC, Chertova E, Keele BF, Bess JW, Jr., Lifson JD, Haslam SM, Dell A, Morris HR.** 2016. Mapping the complete glycoproteome of virion-derived HIV-1 gp120 provides insights into broadly neutralizing antibody binding. Scientific reports **6:**32956.
22. **Behrens AJ, Vasiljevic S, Pritchard LK, Harvey DJ, Andev RS, Krumm SA, Struwe WB, Cupo A, Kumar A, Zitzmann N, Seabright GE, Kramer HB, Spencer DI, Royle L, Lee JH, Klasse PJ, Burton DR, Wilson IA, Ward AB, Sanders RW, Moore JP, Doores KJ, Crispin M.** 2016. Composition and Antigenic Effects of Individual Glycan Sites of a Trimeric HIV-1 Envelope Glycoprotein. Cell Rep **14:**2695-2706.
23. **Kong L, Lee JH, Doores KJ, Murin CD, Julien JP, McBride R, Liu Y, Marozsan A, Cupo A, Klasse PJ, Hoffenberg S, Caulfield M, King CR, Hua Y, Le KM, Khayat R, Deller MC, Clayton T, Tien H, Feizi T, Sanders RW, Paulson JC, Moore JP, Stanfield RL, Burton DR, Ward AB, Wilson IA.** 2013. Supersite of immune vulnerability on the glycosylated face of HIV-1 envelope glycoprotein gp120. Nat Struct Mol Biol **20:**796-803.
24. **Mouquet H, Scharf L, Euler Z, Liu Y, Eden C, Scheid JF, Halper-Stromberg A, Gnanapragasam PN, Spencer DI, Seaman MS, Schuitemaker H, Feizi T, Nussenzweig MC, Bjorkman PJ.** 2012. Complex-type N-glycan recognition by potent broadly neutralizing HIV antibodies. Proceedings of the National Academy of Sciences of the United States of America **109:**E3268-3277.
25. **Pejchal R, Doores KJ, Walker LM, Khayat R, Huang PS, Wang SK, Stanfield RL, Julien JP, Ramos A, Crispin M, Depetris R, Katpally U, Marozsan A, Cupo A, Maloveste S, Liu Y, McBride R, Ito Y, Sanders RW, Ogohara C, Paulson JC, Feizi T, Scanlan CN, Wong CH, Moore JP, Olson WC, Ward AB, Poignard P, Schief WR, Burton DR, Wilson IA.** 2011. A potent and broad neutralizing antibody recognizes and penetrates the HIV glycan shield. Science **334:**1097-1103.

26. **Walker LM, Phogat SK, Chan-Hui PY, Wagner D, Phung P, Goss JL, Wrin T, Simek MD, Fling S, Mitcham JL, Lehrman JK, Priddy FH, Olsen OA, Frey SM, Hammond PW, Kaminsky S, Zamb T, Moyle M, Koff WC, Poignard P, Burton DR.** 2009. Broad and potent neutralizing antibodies from an African donor reveal a new HIV-1 vaccine target. Science **326:**285-289.

27. **Doria-Rose NA, Bhiman JN, Roark RS, Schramm CA, Gorman J, Chuang GY, Pancera M, Cale EM, Ernandes MJ, Louder MK, Asokan M, Bailer RT, Druz A, Fraschilla IR, Garrett NJ, Jarosinski M, Lynch RM, McKee K, O'Dell S, Pegu A, Schmidt SD, Staupe RP, Sutton MS, Wang K, Wibmer CK, Haynes BF, Abdool-Karim S, Shapiro L, Kwong PD, Moore PL, Morris L, Mascola JR.** 2015. New Member of the V1V2-Directed CAP256-VRC26 Lineage That Shows Increased Breadth and Exceptional Potency. J Virol **90:**76-91.

28. **Bonsignori M, Hwang KK, Chen X, Tsao CY, Morris L, Gray E, Marshall DJ, Crump JA, Kapiga SH, Sam NE, Sinangil F, Pancera M, Yongping Y, Zhang B, Zhu J, Kwong PD, O'Dell S, Mascola JR, Wu L, Nabel GJ, Phogat S, Seaman MS, Whitesides JF, Moody MA, Kelsoe G, Yang X, Sodroski J, Shaw GM, Montefiori DC, Kepler TB, Tomaras GD, Alam SM, Liao HX, Haynes BF.** 2011. Analysis of a clonal lineage of HIV-1 envelope V2/V3 conformational epitope-specific broadly neutralizing antibodies and their inferred unmutated common ancestors. Journal of virology **85:**9998-10009.

29. **Falkowska E, Le KM, Ramos A, Doores KJ, Lee JH, Blattner C, Ramirez A, Derking R, van Gils MJ, Liang CH, McBride R, von Bredow B, Shivatare SS, Wu CY, Chan-Hui PY, Liu Y, Feizi T, Zwick MB, Koff WC, Seaman MS, Swiderek K, Moore JP, Evans D, Paulson JC, Wong CH, Ward AB, Wilson IA, Sanders RW, Poignard P, Burton DR.** 2014. Broadly Neutralizing HIV Antibodies Define a Glycan-Dependent Epitope on the Prefusion Conformation of gp41 on Cleaved Envelope Trimers. Immunity **40:**657-668.

30. **Huang J, Kang BH, Pancera M, Lee JH, Tong T, Feng Y, Imamichi H, Georgiev IS, Chuang GY, Druz A, Doria-Rose NA, Laub L, Sliepen K, van Gils MJ, de la Pena AT, Derking R, Klasse PJ, Migueles SA, Bailer RT, Alam M, Pugach P, Haynes BF, Wyatt RT, Sanders RW, Binley JM, Ward AB, Mascola JR, Kwong PD, Connors M.** 2014. Broad and potent HIV-1 neutralization by a human antibody that binds the gp41-gp120 interface. Nature **515:**138-142.

31. **Scharf L, Scheid JF, Lee JH, West AP, Jr., Chen C, Gao H, Gnanapragasam PN, Mares R, Seaman MS, Ward AB, Nussenzweig MC, Bjorkman PJ.** 2014. Antibody 8ANC195 reveals a site of broad vulnerability on the HIV-1 envelope spike. Cell Rep **7:**785-795.

32. **Binley JM, Ban YE, Crooks ET, Eggink D, Osawa K, Schief WR, Sanders RW.** 2010. Role of complex carbohydrates in human immunodeficiency virus type 1 infection and resistance to antibody neutralization. Journal of virology **84:**5637-5655.

33. **Kim AS, Leaman DP, Zwick MB.** 2014. Antibody to gp41 MPER alters functional properties of HIV-1 Env without complete neutralization. PLoS pathogens **10:**e1004271.

34. **Reitter JN, Means RE, Desrosiers RC.** 1998. A role for carbohydrates in immune evasion in AIDS. Nat Med **4:**679-684.

35. **Moore PL, Gray ES, Wibmer CK, Bhiman JN, Nonyane M, Sheward DJ, Hermanus T, Bajimaya S, Tumba NL, Abrahams MR, Lambson BE, Ranchobe N, Ping L, Ngandu N, Abdool Karim Q, Abdool Karim SS, Swanstrom RI, Seaman MS, Williamson C, Morris L.** 2012. Evolution of an HIV glycan-dependent broadly neutralizing antibody epitope through immune escape. Nature medicine **18:**1688-1692.

36. **Gao F, Bonsignori M, Liao HX, Kumar A, Xia SM, Lu X, Cai F, Hwang KK, Song H, Zhou T, Lynch RM, Alam SM, Moody MA, Ferrari G, Berrong M, Kelsoe G, Shaw GM, Hahn BH, Montefiori DC, Kamanga G, Cohen MS, Hraber P, Kwong PD, Korber BT, Mascola JR, Kepler TB, Haynes BF.** 2014. Cooperation of B Cell Lineages in Induction of HIV-1-Broadly Neutralizing Antibodies. Cell **158:**481-491.
37. **Wibmer CK, Bhiman JN, Gray ES, Tumba N, Abdool Karim SS, Williamson C, Morris L, Moore PL.** 2013. Viral escape from HIV-1 neutralizing antibodies drives increased plasma neutralization breadth through sequential recognition of multiple epitopes and immunotypes. PLoS pathogens **9:**e1003738.
38. **McGuire AT, Hoot S, Dreyer AM, Lippy A, Stuart A, Cohen KW, Jardine J, Menis S, Scheid JF, West AP, Schief WR, Stamatatos L.** 2013. Engineering HIV envelope protein to activate germline B cell receptors of broadly neutralizing anti-CD4 binding site antibodies. The Journal of experimental medicine **210:**655-663.
39. **Derdeyn CA, Decker JM, Bibollet-Ruche F, Mokili JL, Muldoon M, Denham SA, Heil ML, Kasolo F, Musonda R, Hahn BH, Shaw GM, Korber BT, Allen S, Hunter E.** 2004. Envelope-constrained neutralization-sensitive HIV-1 after heterosexual transmission. Science **303:**2019-2022.
40. **Chohan B, Lang D, Sagar M, Korber B, Lavreys L, Richardson B, Overbaugh J.** 2005. Selection for human immunodeficiency virus type 1 envelope glycosylation variants with shorter V1-V2 loop sequences occurs during transmission of certain genetic subtypes and may impact viral RNA levels. J Virol **79:**6528-6531.
41. **Edo-Matas D, Rachinger A, Setiawan LC, Boeser-Nunnink BD, van 't Wout AB, Lemey P, Schuitemaker H.** 2012. The evolution of human immunodeficiency virus type-1 (HIV-1) envelope molecular properties and coreceptor use at all stages of infection in an HIV-1 donor-recipient pair. Virology **422:**70-80.
42. **Parrish NF, Gao F, Li H, Giorgi EE, Barbian HJ, Parrish EH, Zajic L, Iyer SS, Decker JM, Kumar A, Hora B, Berg A, Cai F, Hopper J, Denny TN, Ding H, Ochsenbauer C, Kappes JC, Galimidi RP, West AP, Jr., Bjorkman PJ, Wilen CB, Doms RW, O'Brien M, Bhardwaj N, Borrow P, Haynes BF, Muldoon M, Theiler JP, Korber B, Shaw GM, Hahn BH.** 2013. Phenotypic properties of transmitted founder HIV-1. Proc Natl Acad Sci U S A **110:**6626-6633.
43. **Samleerat T, Braibant M, Jourdain G, Moreau A, Ngo-Giang-Huong N, Leechanachai P, Hemvuttiphan J, Hinjiranandana T, Changchit T, Warachit B, Suraseranivong V, Lallemant M, Barin F.** 2008. Characteristics of HIV type 1 (HIV-1) glycoprotein 120 env sequences in mother-infant pairs infected with HIV-1 subtype CRF01_AE. J Infect Dis **198:**868-876.
44. **Curlin ME, Zioni R, Hawes SE, Liu Y, Deng W, Gottlieb GS, Zhu T, Mullins JI.** 2010. HIV-1 envelope subregion length variation during disease progression. PLoS pathogens **6:**e1001228.
45. **Bunnik EM, Pisas L, van Nuenen AC, Schuitemaker H.** 2008. Autologous neutralizing humoral immunity and evolution of the viral envelope in the course of subtype B human immunodeficiency virus type 1 infection. Journal of virology **82:**7932-7941.
46. **Chackerian B, Rudensey LM, Overbaugh J.** 1997. Specific N-linked and O-linked glycosylation modifications in the envelope V1 domain of simian immunodeficiency virus variants that evolve in the host alter recognition by neutralizing antibodies. J Virol **71:**7719-7727.
47. **Back NK, Smit L, De Jong JJ, Keulen W, Schutten M, Goudsmit J, Tersmette M.** 1994. An N-glycan within the human immunodeficiency virus type 1 gp120 V3 loop affects virus neutralization. Virology **199:**431-438.
48. **Doria-Rose NA, Schramm CA, Gorman J, Moore PL, Bhiman JN, DeKosky BJ, Ernandes MJ, Georgiev IS, Kim HJ, Pancera M, Staupe RP, Altae-Tran HR,**

Bailer RT, Crooks ET, Cupo A, Druz A, Garrett NJ, Hoi KH, Kong R, Louder MK, Longo NS, McKee K, Nonyane M, O'Dell S, Roark RS, Rudicell RS, Schmidt SD, Sheward DJ, Soto C, Wibmer CK, Yang Y, Zhang Z, Mullikin JC, Binley JM, Sanders RW, Wilson IA, Moore JP, Ward AB, Georgiou G, Williamson C, Abdool Karim SS, Morris L, Kwong PD, Shapiro L, Mascola JR. 2014. Developmental pathway for potent V1V2-directed HIV-neutralizing antibodies. Nature **509:**55-62.

49. **Moore PL, Sheward D, Nonyane M, Ranchobe N, Hermanus T, Gray ES, Abdool Karim SS, Williamson C, Morris L.** 2013. Multiple pathways of escape from HIV broadly cross-neutralizing V2-dependent antibodies. Journal of virology **87:**4882-4894.

50. **Aricescu AR, Lu W, Jones EY.** 2006. A time- and cost-efficient system for high-level protein production in mammalian cells. Acta Crystallogr D Biol Crystallogr **62:**1243-1250.

51. **Dunlop DC, Bonomelli C, Mansab F, Vasiljevic S, Doores KJ, Wormald MR, Palma AS, Feizi T, Harvey DJ, Dwek RA, Crispin M, Scanlan CN.** 2010. Polysaccharide mimicry of the epitope of the broadly neutralizing anti-HIV antibody, 2G12, induces enhanced antibody responses to self oligomannose glycans. Glycobiology **20:**812-823.

52. **Royle L, Radcliffe CM, Dwek RA, Rudd PM.** 2006. Detailed structural analysis of N-glycans released from glycoproteins in SDS-PAGE gel bands using HPLC combined with exoglycosidase array digestions. Methods in molecular biology **347:**125-143.

53. **Neville DC, Dwek RA, Butters TD.** 2009. Development of a single column method for the separation of lipid- and protein-derived oligosaccharides. J Proteome Res **8:**681-687.

54. **Li M, Gao F, Mascola JR, Stamatatos L, Polonis VR, Koutsoukos M, Voss G, Goepfert P, Gilbert P, Greene KM, Bilska M, Kothe DL, Salazar-Gonzalez JF, Wei X, Decker JM, Hahn BH, Montefiori DC.** 2005. Human immunodeficiency virus type 1 env clones from acute and early subtype B infections for standardized assessments of vaccine-elicited neutralizing antibodies. J Virol **79:**10108-10125.

55. **Montefiori DC.** 2005. Evaluating neutralizing antibodies against HIV, SIV, and SHIV in luciferase reporter gene assays. Curr Protoc Immunol **Chapter 12:**Unit 12 11.

56. **Moore PL, Gray ES, Choge IA, Ranchobe N, Mlisana K, Abdool Karim SS, Williamson C, Morris L, Team CS.** 2008. The c3-v4 region is a major target of autologous neutralizing antibodies in human immunodeficiency virus type 1 subtype C infection. J Virol **82:**1860-1869.

57. **Bhiman JN, Anthony C, Doria-Rose NA, Karimanzira O, Schramm CA, Khoza T, Kitchin D, Botha G, Gorman J, Garrett NJ, Abdool Karim SS, Shapiro L, Williamson C, Kwong PD, Mascola JR, Morris L, Moore PL.** 2015. Viral variants that initiate and drive maturation of V1V2-directed HIV-1 broadly neutralizing antibodies. Nat Med **21:**1332-1336.

58. **Julien JP, Cupo A, Sok D, Stanfield RL, Lyumkis D, Deller MC, Klasse PJ, Burton DR, Sanders RW, Moore JP, Ward AB, Wilson IA.** 2013. Crystal structure of a soluble cleaved HIV-1 envelope trimer. Science **342:**1477-1483.

59. **Julien JP, Lee JH, Cupo A, Murin CD, Derking R, Hoffenberg S, Caulfield MJ, King CR, Marozsan AJ, Klasse PJ, Sanders RW, Moore JP, Wilson IA, Ward AB.** 2013. Asymmetric recognition of the HIV-1 trimer by broadly neutralizing antibody PG9. Proceedings of the National Academy of Sciences of the United States of America **110:**4351-4356.

60. **Go EP, Hewawasam G, Liao HX, Chen H, Ping LH, Anderson JA, Hua DC, Haynes BF, Desaire H.** 2011. Characterization of glycosylation profiles of HIV-1

transmitted/founder envelopes by mass spectrometry. Journal of virology **85:**8270-8284.

61. **Pancera M, Zhou T, Druz A, Georgiev IS, Soto C, Gorman J, Huang J, Acharya P, Chuang GY, Ofek G, Stewart-Jones GB, Stuckey J, Bailer RT, Joyce MG, Louder MK, Tumba N, Yang Y, Zhang B, Cohen MS, Haynes BF, Mascola JR, Morris L, Munro JB, Blanchard SC, Mothes W, Connors M, Kwong PD.** 2014. Structure and immune recognition of trimeric pre-fusion HIV-1 Env. Nature **514:**455-461.

62. **Gray ES, Moore PL, Pantophlet RA, Morris L.** 2007. N-linked glycan modifications in gp120 of human immunodeficiency virus type 1 subtype C render partial sensitivity to 2G12 antibody neutralization. J Virol **81:**10769-10776.

63. **Sanders RW, Venturi M, Schiffner L, Kalyanaraman R, Katinger H, Lloyd KO, Kwong PD, Moore JP.** 2002. The mannose-dependent epitope for neutralizing antibody 2G12 on human immunodeficiency virus type 1 glycoprotein gp120. J Virol **76:**7293-7305.

64. **Pritchard LK, Spencer DI, Royle L, Vasiljevic S, Krumm SA, Doores KJ, Crispin M.** 2015. Glycan microheterogeneity at the PGT135 antibody recognition site on HIV-1 gp120 reveals a molecular mechanism for neutralization resistance. Journal of virology.

65. **Geijtenbeek TB, Kwon DS, Torensma R, van Vliet SJ, van Duijnhoven GC, Middel J, Cornelissen IL, Nottet HS, KewalRamani VN, Littman DR, Figdor CG, van Kooyk Y.** 2000. DC-SIGN, a dendritic cell-specific HIV-1-binding protein that enhances trans-infection of T cells. Cell **100:**587-597.

66. **Hong PW, Flummerfelt KB, de Parseval A, Gurney K, Elder JH, Lee B.** 2002. Human immunodeficiency virus envelope (gp120) binding to DC-SIGN and primary dendritic cells is carbohydrate dependent but does not involve 2G12 or cyanovirin binding sites: implications for structural analyses of gp120-DC-SIGN binding. J Virol **76:**12855-12865.

67. **Kwon DS, Gregorio G, Bitton N, Hendrickson WA, Littman DR.** 2002. DC-SIGN-mediated internalization of HIV is required for trans-enhancement of T cell infection. Immunity **16:**135-144.

68. **Shen R, Raska M, Bimczok D, Novak J, Smith PD.** 2014. HIV-1 envelope glycan moieties modulate HIV-1 transmission. J Virol **88:**14258-14267.

69. **Banerjee K, Andjelic S, Klasse PJ, Kang Y, Sanders RW, Michael E, Durso RJ, Ketas TJ, Olson WC, Moore JP.** 2009. Enzymatic removal of mannose moieties can increase the immune response to HIV-1 gp120 in vivo. Virology **389:**108-121.

70. **Banerjee K, Michael E, Eggink D, van Montfort T, Lasnik AB, Palmer KE, Sanders RW, Moore JP, Klasse PJ.** 2012. Occluding the mannose moieties on human immunodeficiency virus type 1 gp120 with griffithsin improves the antibody responses to both proteins in mice. AIDS Res Hum Retroviruses **28:**206-214.

71. **Kong L, Sheppard NC, Stewart-Jones GB, Robson CL, Chen H, Xu X, Krashias G, Bonomelli C, Scanlan CN, Kwong PD, Jeffs SA, Jones IM, Sattentau QJ.** 2010. Expression-system-dependent modulation of HIV-1 envelope glycoprotein antigenicity and immunogenicity. J Mol Biol **403:**131-147.

72. **Lee JH, de Val N, Lyumkis D, Ward AB.** 2015. Model Building and Refinement of a Natively Glycosylated HIV-1 Env Protein by High-Resolution Cryoelectron Microscopy. Structure.

All sequences

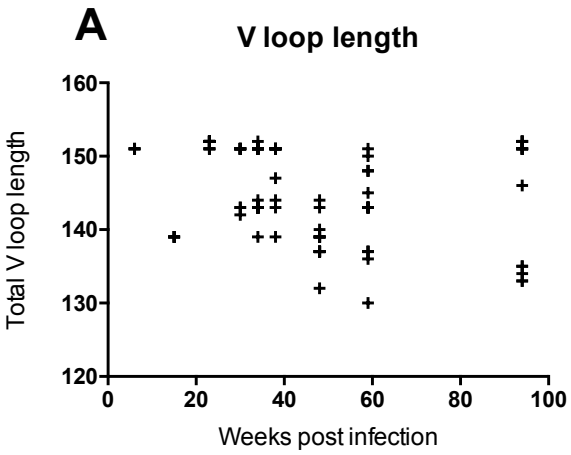

All: r= -0.1263, p=0.1249
To wk94: r= -0.2496, p=0.0039

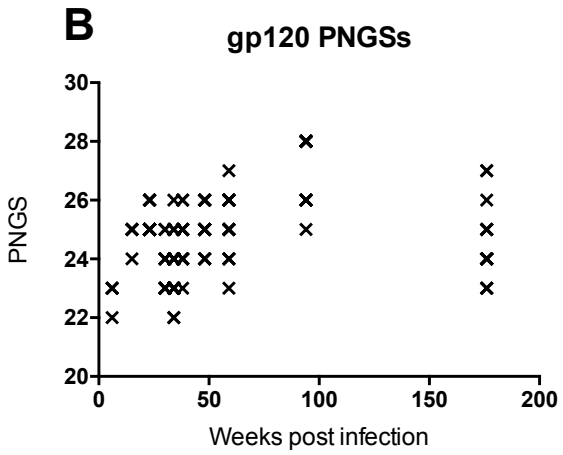

All: r=0.2106, p=0.0099
To wk94: r=0.6412, p<0.0001

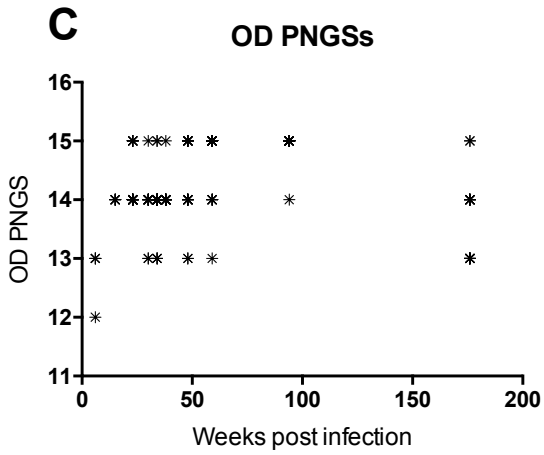

All: r=0.003, p=0.97
To w94: r=0.5651, p<0.0001

Expressed gp120s

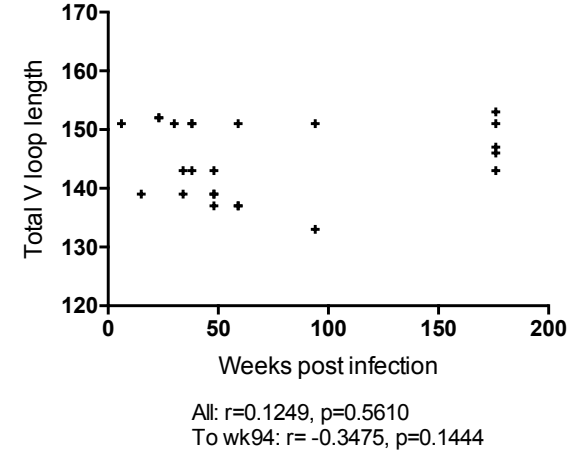

All: r=0.1249, p=0.5610
To wk94: r= -0.3475, p=0.1444

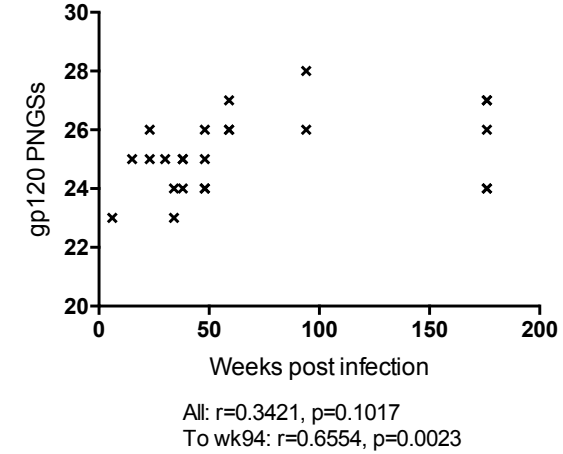

All: r=0.3421, p=0.1017
To wk94: r=0.6554, p=0.0023

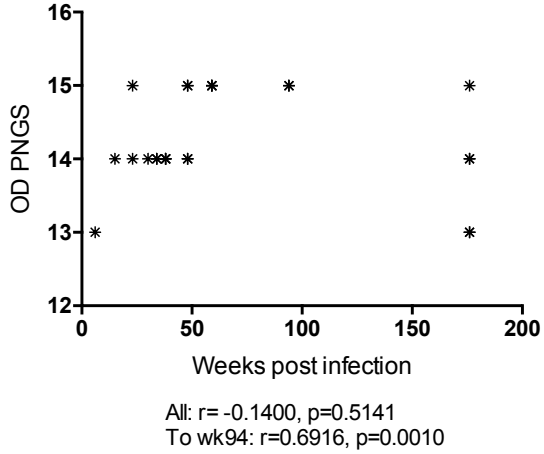

All: r= -0.1400, p=0.5141
To wk94: r=0.6916, p=0.0010

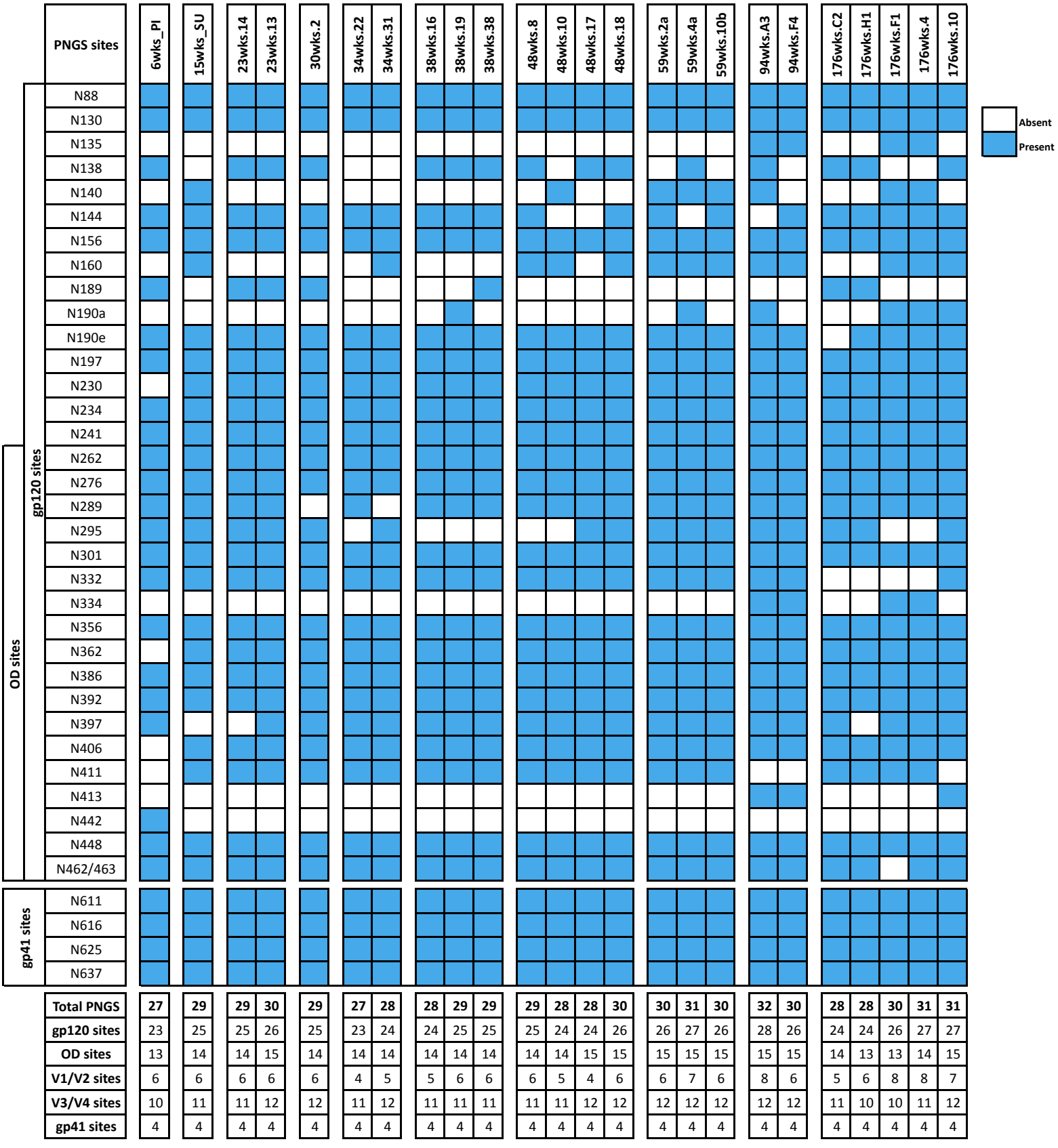
PNGS sites
6wks_PI
15wks_SU
23wks.14
23wks.13
30wks.2
34wks.22
34wks.31
38wks.16
38wks.19
38wks.38
48wks.8
48wks.10
48wks.17
48wks.18
59wks.2a
59wks.4a
59wks.10b
94wks.A3
94wks.F4
176wks.C2
176wks.H1
176wks.F1
176wks.4
176wks.10
OD sites
gp120 sites
gp41 sites
N88
N130
N135
N138
N140
N144
N156
N160
N189
N190a
N190e
N197
N230
N234
N241
N262
N276
N289
N295
N301
N332
N334
N356
N362
N386
N392
N397
N406
N411
N413
N442
N448
N462/463
N611
N616
N625
N637
Absent
Present
Total PNGS 27 29 29 30 29 27 28 28 29 29 29 28 28 30 30 31 30 32 30 28 28 30 31 31
gp120 sites 23 25 25 26 25 23 24 24 25 25 25 24 24 26 26 27 26 28 26 24 24 26 27 27
OD sites 13 14 14 15 14 14 14 14 14 14 14 14 15 15 15 15 15 15 15 14 13 13 14 15
V1/V2 sites 6 6 6 6 6 4 5 5 6 6 6 5 4 6 6 7 6 8 6 5 6 8 8 7
V3/V4 sites 10 11 11 12 12 11 12 11 11 11 11 11 12 12 12 12 12 12 12 11 10 10 11 12
gp41 sites 4 4 4 4 4 4 4 4 4 4 4 4 4 4 4 4 4 4 4 4 4 4 4 4

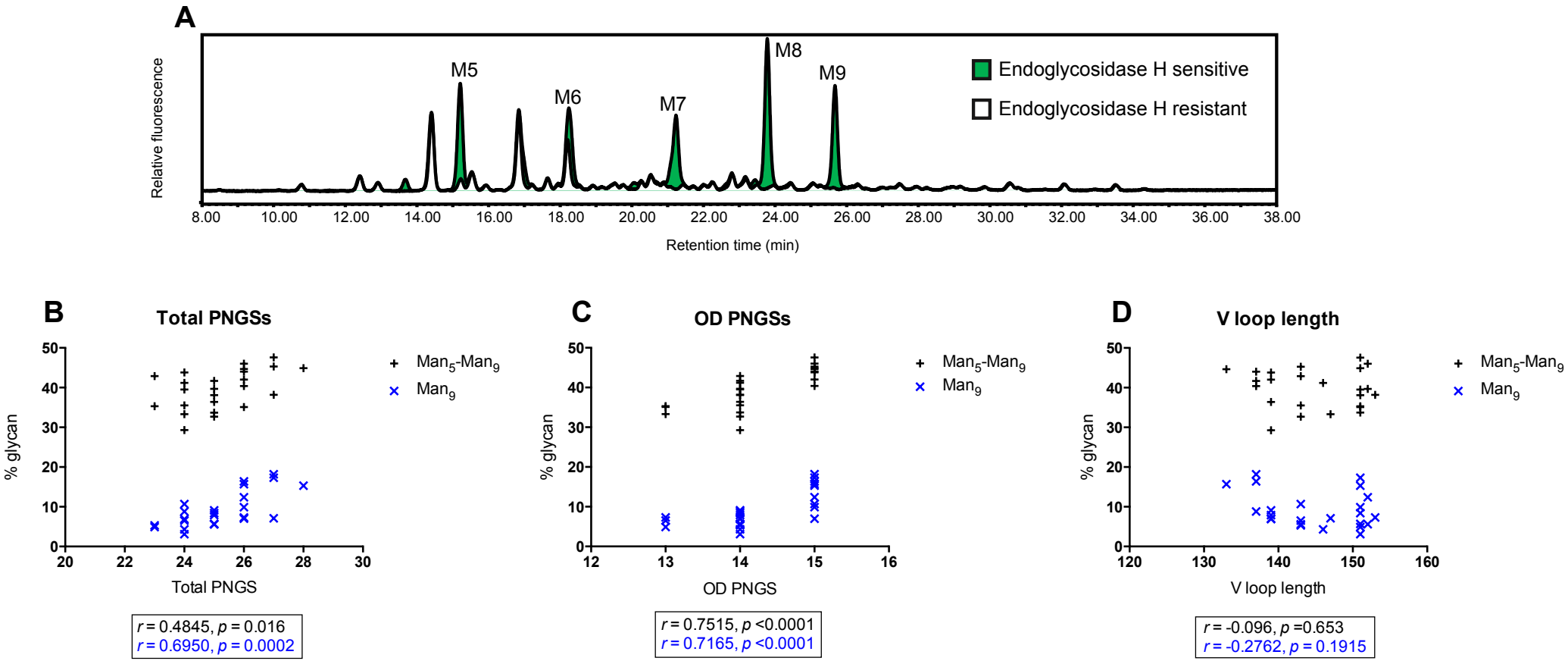
A
Relative fluorescence
M5
M6
M7
M8
M9
Endoglycosidase H sensitive
Endoglycosidase H resistant
8.00
10.00
12.00
14.00
16.00
18.00
20.00
22.00
24.00
26.00
28.00
30.00
32.00
34.00
36.00
38.00
Retention time (min)
B
Total PNGSs
% glycan
Man5-Man9
Man9
Total PNGS
r = 0.4845, p = 0.016
r = 0.6950, p = 0.0002
C
OD PNGSs
% glycan
Man5-Man9
Man9
OD PNGS
r = 0.7515, p <0.0001
r = 0.7165, p <0.0001
D
V loop length
% glycan
Man5-Man9
Man9
V loop length
r = -0.096, p =0.653
r = -0.2762, p = 0.1915

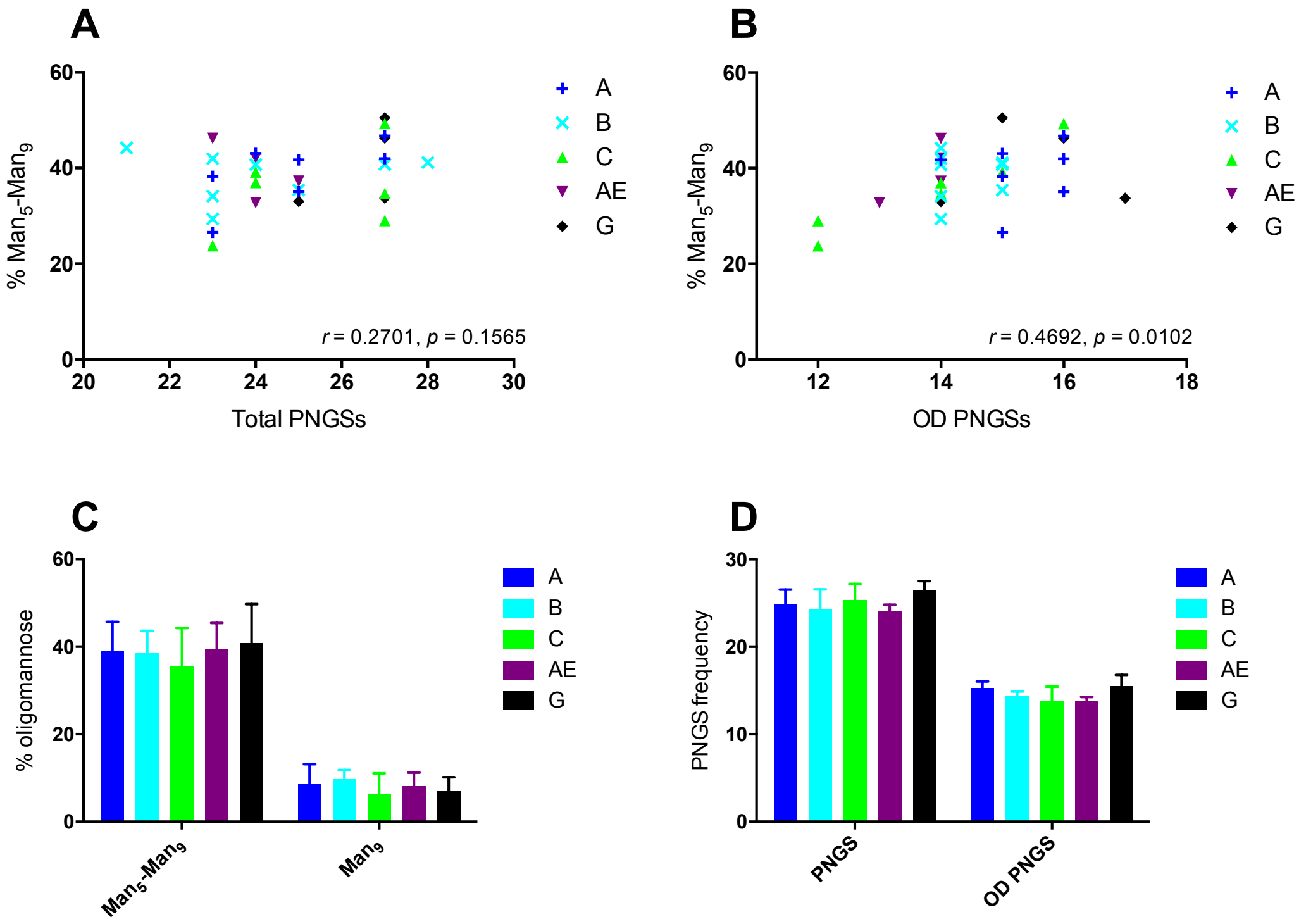
A
% Man5-Man9
Total PNGSs
r = 0.2701, p = 0.1565
A
B
C
AE
G
B
% Man5-Man9
OD PNGSs
r = 0.4692, p = 0.0102
C
% oligomannose
Man5-Man9
Man9
D
PNGS frequency
PNGS
OD PNGS

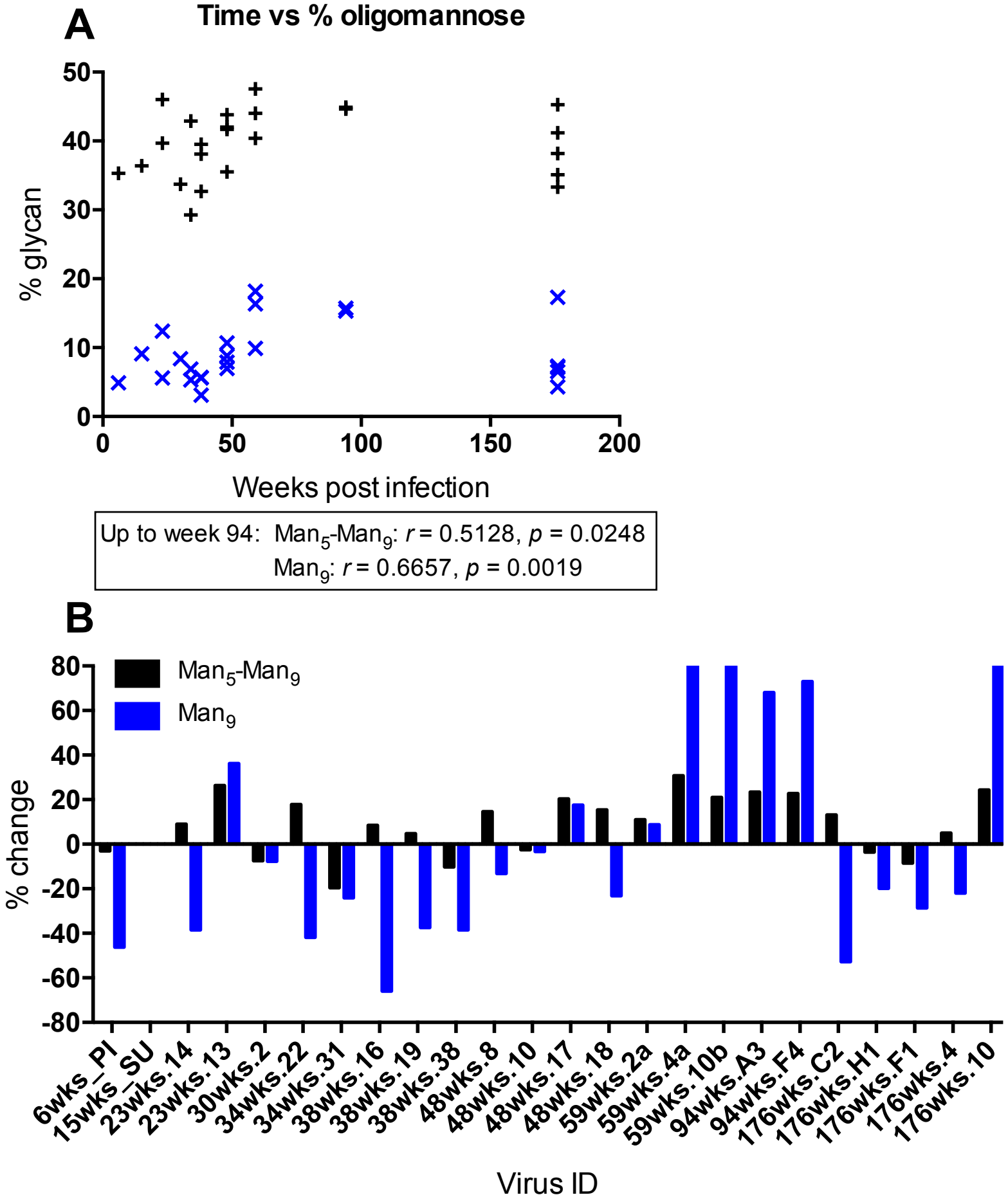
A
Time vs % oligomannose
% glycan
Weeks post infection
Up to week 94: Man5-Man9: r = 0.5128, p = 0.0248
Man9: r = 0.6657, p = 0.0019
B
Man5-Man9
Man9
% change
6wks_PI
15wks_SU
23wks.14
23wks.13
30wks.2
34wks.22
34wks.31
38wks.16
38wks.19
38wks.38
48wks.8
48wks.10
48wks.17
48wks.18
59wks.2a
59wks.4a
59wks.10b
94wks.A3
94wks.F4
176wks.C2
176wks.H1
176wks.F1
176wks.4
176wks.10
Virus ID

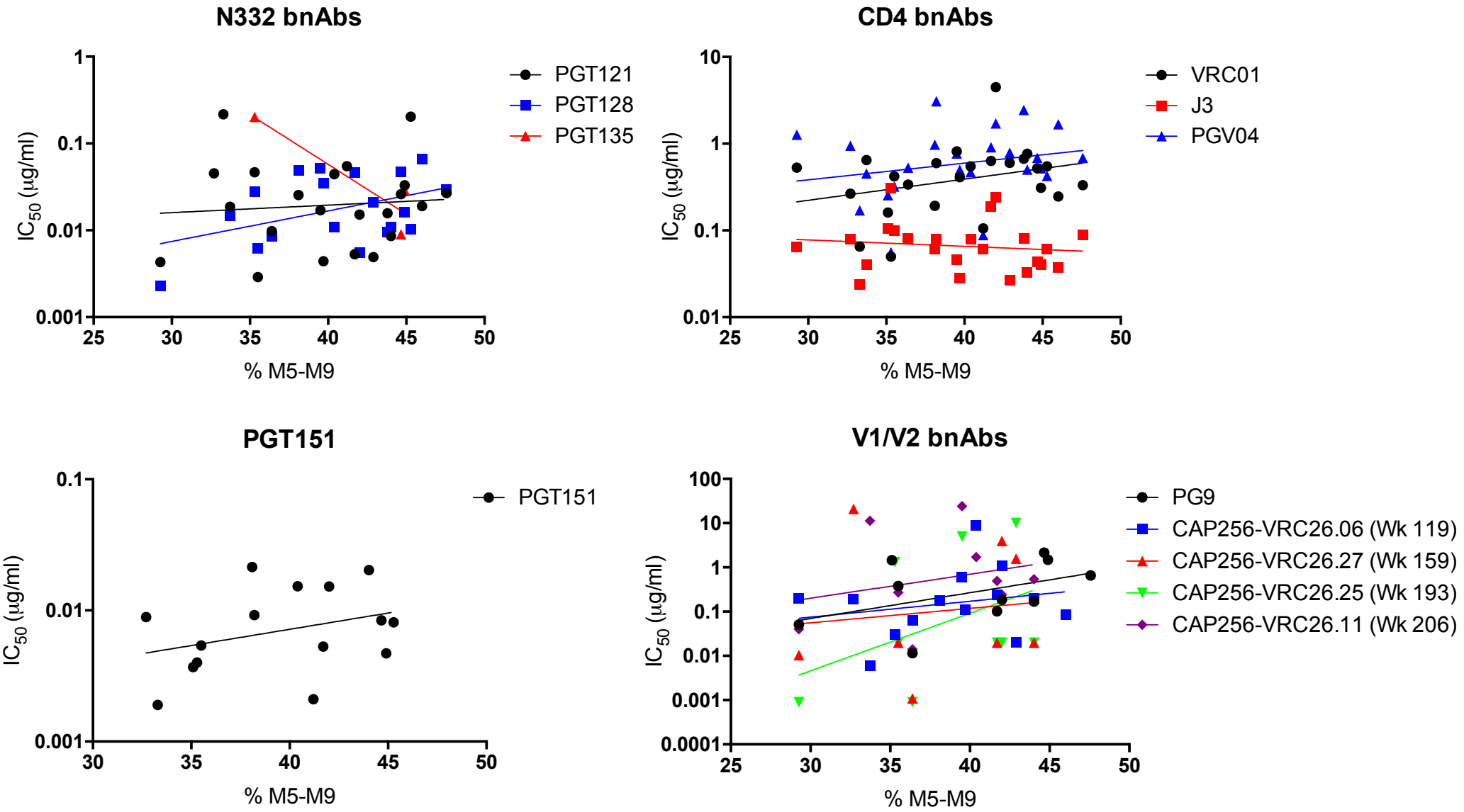
N332 bnAbs
IC50 (µg/ml)
% M5-M9
PGT121
PGT128
PGT135
CD4 bnAbs
VRC01
J3
PGV04
PGT151
PGT151
V1/V2 bnAbs
PG9
CAP256-VRC26.06 (Wk 119)
CAP256-VRC26.27 (Wk 159)
CAP256-VRC26.25 (Wk 193)
CAP256-VRC26.11 (Wk 206)

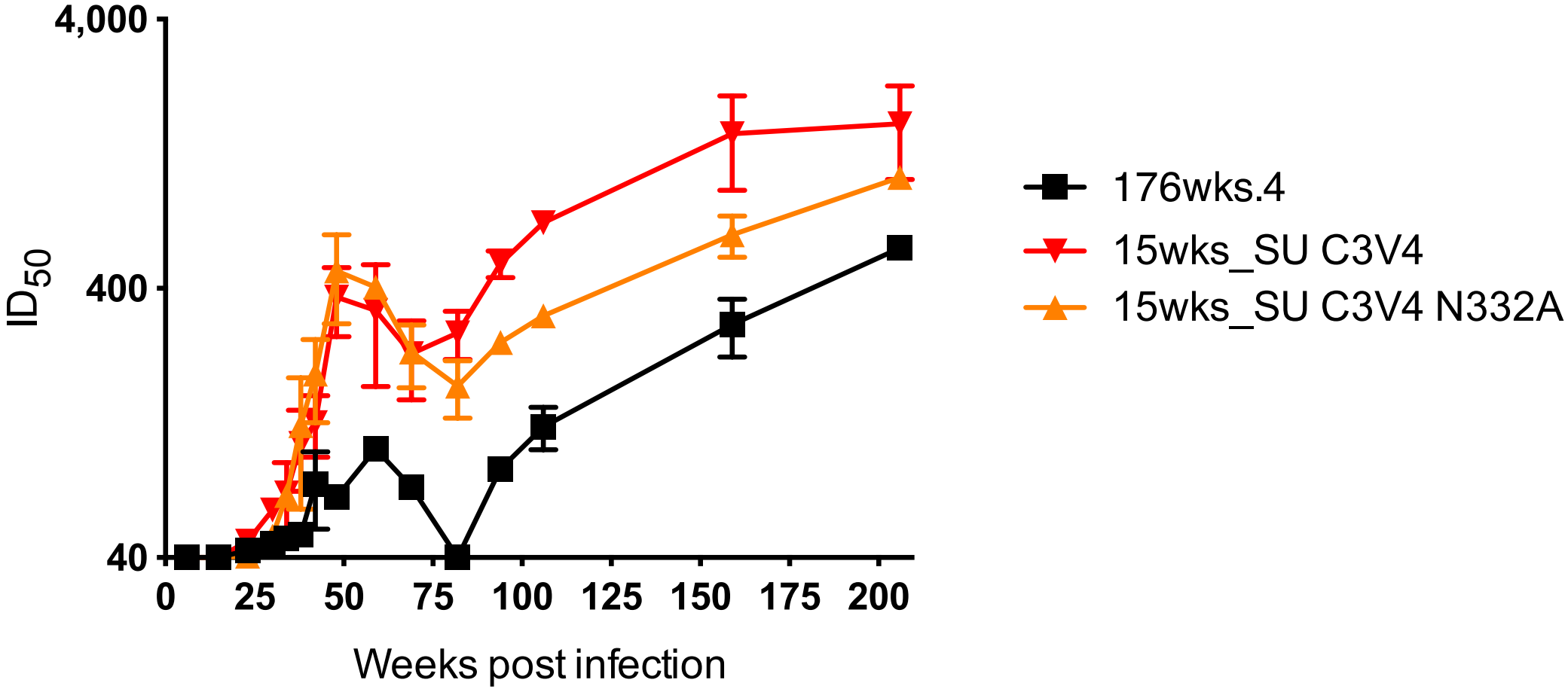
4,000
400
40
ID50
0
25
50
75
100
125
150
175
200
Weeks post infection
176wks.4
15wks_SU C3V4
15wks_SU C3V4 N332A

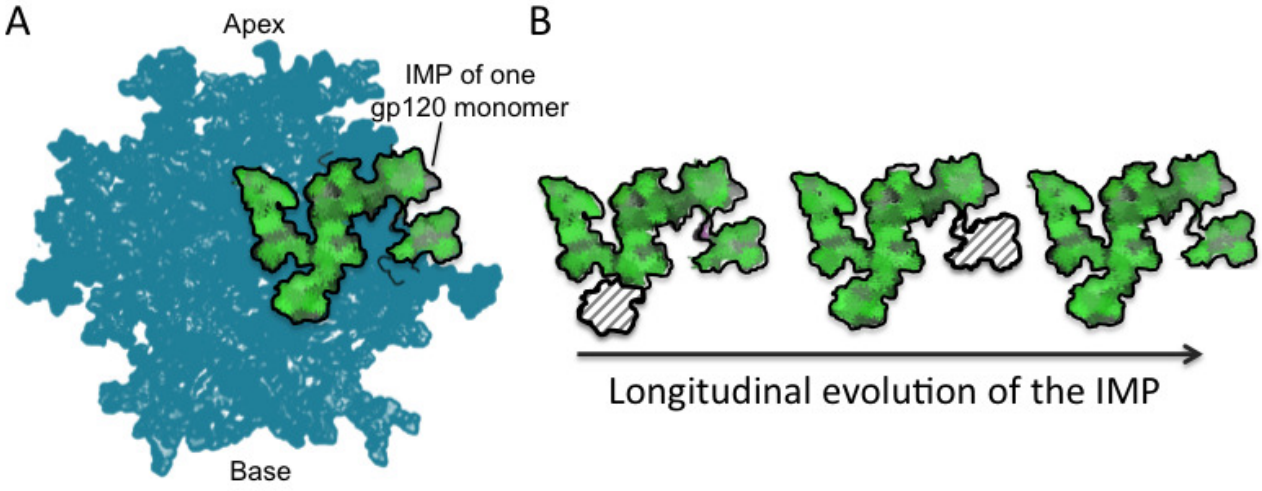
A
Apex
IMP of one
gp120 monomer
Base
B
Longitudinal evolution of the IMP